ACS Catalysis

Letter

pubs.acs.org/acscatalysis

Size-Dependent Sulfur Poisoning of Silica-Supported Monodisperse Pt Nanoparticle Hydrogenation Catalysts

Lyndsey M. Baldyga,[†] Selasi O. Blavo,[†] Chun-Hong Kuo,[‡] Chia-Kuang Tsung,[‡] and John N. Kuhn*,[†]

[†]Department of Chemical & Biomedical Engineering, University of South Florida, 4202 East Fowler Avenue, ENB 118, Tampa, Florida 33620, United States

[‡]Department of Chemistry, Boston College, Chestnut Hill, Massachusetts 02467, United States

Supporting Information

ABSTRACT: Colloidal techniques were used to synthesize monodisperse Pt nanoparticles of four distinct sizes between 2 and 7 nm before immobilization onto silica. Ethylene hydrogenation demonstrated structure-insensitive behavior with TOFs of ~12 s^{-1} before poisoning. With thiophene being a strong binding adsorbate, TOFs decreased by orders of magnitude, and the poisoning-induced antipathetic structure sensitivity because thiophene adsorbed more strongly to the coordinatively unsaturated, as compared with coordinatively saturated, surfaces, and the degree of saturation increased with decreasing Pt size. This effort is part of a broader study in which structure sensitivity is analyzed for adsorbates in complex reaction networks.

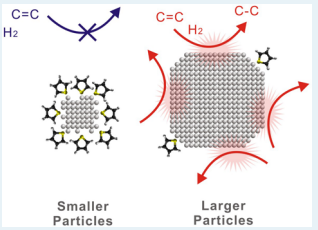

KEYWORDS: *platinum, sulfur poisoning, colloidal synthesis with size control, structure sensitivity*

1. INTRODUCTION

Since sulfur is a well known environmental contaminant and poison in catalytic processes,[1] challenges exist in finding effective catalysts for conversion processes involving this problematic element. For hydrodesulfurization (HDS) in fuel processing, two general strategies exist. First, sulfided catalysts, such as cobalt−molybdenum (CoMo) or nickel−molybdenum (NiMo) supported on γ-alumina are used. These catalysts operate well in high concentrations of sulfur because the active phase is a sulfide.[2] Alternatively, precious metal catalysts (e.g., Pt[3]) efficiently remove lower concentrations of sulfur, but poison at high sulfur concentrations. As sulfur emission regulations become increasingly stringent, two reactors in series, with a sulfided catalyst in the first and a metal one in the second reactor, have been proposed to meet requirements for ultraclean fuels.[4−7]

Another noteworthy difference between base metal sulfides and precious metal catalysts is the reaction mechanism. Whereas the base metal sulfides can catalyze both the direct desulfurization and desulfurization by hydrogenation, the hydrogenation route is dominant for precious metals.[8−10] Moreover, for use in the second reactor to achieve deep desulfurization, sulfur is mostly contained in refractory molecules (e.g., 4,6 dimethylbenzothiophene[11]), in which alkyl groups provide steric hindrance to prevent direct desulfurization.[12]

Previous studies have identified various particle sizes of precious metal catalysts as being optimal for HDS by hydrogenation. Through extensive characterization following sulfidation, Matsui et al.[13] concluded that Pt particles immobilized on high-silica USY zeolites of sizes smaller than 2 nm were more sulfur-tolerant than larger particles. Another study[14] determined alumina and silica−alumina-supported Pt particles of 1.2 nm in size were more active than larger Pt particles for conversion of 4-ethyl, 6-methyldibenzothiophene (4-E,6MDBT) because the reaction proceeds over sulfur vacancies on the surfaces of the particles, which are more prevalent in small particles. Alternatively, Wang and Iglesia[8] demonstrated increasing turnover rates for thiophene hydrodesulfurization on Pt/silica with the Pt particle size increasing from 2 to 8 nm and related the trend to increasing surface vacancy densities with increasing particle size (i.e., strong sulfur binding for the coordinatively unsaturated surfaces of the small particles). These authors made a similar conclusion from similar work on silica-supported Ru particles.[15] The results of these studies are complicated by the use of different supports,[16,17] which, along with cofeeding basic molecules to reduce the impact of acidic supports,[18] may be the source of discrepancies. None of the studies in the literature use well-defined metal particle morphologies, as the current study does, which may provide an attractive route for designing catalysts with high sulfur tolerance.

The focus of the current work is to present a fundamental examination on the structure sensitivity of Pt's sulfur poisoning for hydrogenation catalysis. The approach is to synthesize monodisperse Pt nanoparticles of different sizes using colloidal synthesis and immobilize the particles onto silica, which is a support that minimizes the metal−support interactions, allowing for isolation of the metal functionality. The size dependence of poisoning is then determined using ethylene hydrogenation as the activity measure with and without sulfur treatments prior to the catalysis.

Received: September 21, 2012
Revised: October 26, 2012

   dx.doi.org/10.1021/cs300625m | *ACS Catal.* 2012, 2, 2626−2629

2. RESULTS AND DISCUSSION

2.1. Synthesis and Characterization of Pt/Silica Heterogeneous Catalysts. The Pt particles after washing but before immobilization onto silica are compared at the same magnification (10 nm scale bars) in Figure 1. The smallest

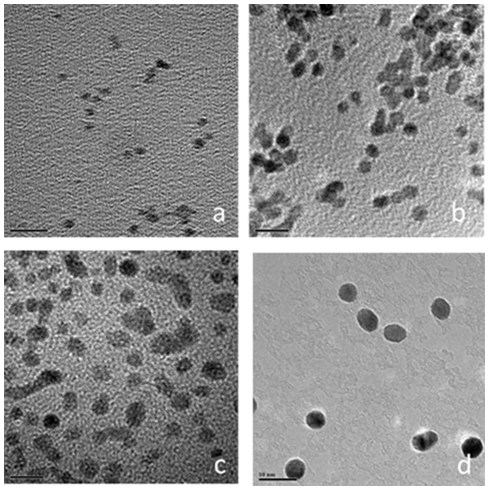

Figure 1. Representative TEM images. All scale bars are 10 nm. (a) 2.0, (b) 3.4, (c) 4.3, and (d) 6.8 nm Pt particles.

particles (Figure 1a) were 2.0 nm, which was in agreement with previous studies using this synthesis.[19,20] These particles are synthesized at higher temperature (155 °C), allowing for quick nucleation, which leads to uniform and small-size particles. The highly basic condition stabilizes the surface with hydroxyl ligands prior to neutralization and addition of the polymer capping. The three particles with larger sizes are synthesized with the assistance of the seeds from the lower temperature (110 °C) synthesis. The lower temperature limits nucleation and permits only the overgrowth on the seeds that yields the ability to control particle size. Similar to a previous report,[21] additional Pt precursor was added to the 3.4 nm seeds (Figure 1b) to control the particle size in the 3.4 nm-plus size range (Figure 1c and d). For all particles, the average particle size and related size distribution (from TEM) and the corresponding dispersion based on the size are presented in Table 1.

Table 1. Particle Size Distributions from Statistical Analysis of TEM Images and Dispersion Using %D = 110/size(nm)

size (nm)	dispersion (%)
2.0 ± 0.4	55.0
3.4 ± 0.6	32.4
4.3 ± 0.7	25.6
6.8 ± 0.9	16.2

After immobilization of the washed Pt particles onto silica (Cab-O-Sil; ~210 m^2/g) at a 1% loading by Pt mass, TEM images (4.3 nm Pt/silica catalyst, Figure 2) were used to demonstrate distribution of the nanoparticles across the surface of the silica and maintenance of the particle sizes. Then TPO experiments (Figure 3) were conducted with the 2.0 nm Pt/silica catalysts to demonstrate the effective removal by washing of the polymer capping used to stabilize the particles before the immobilization. As presented in Figure 3a, no oxygen consumption (m/z = 32) or combustion products were

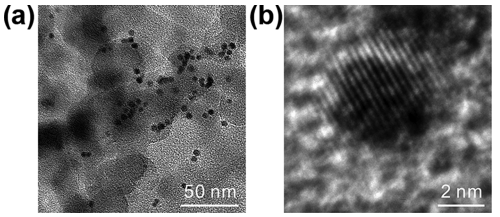

Figure 2. TEM images of the 5 nm Pt/silica catalyst after immobilization of the nanoparticles into the support.

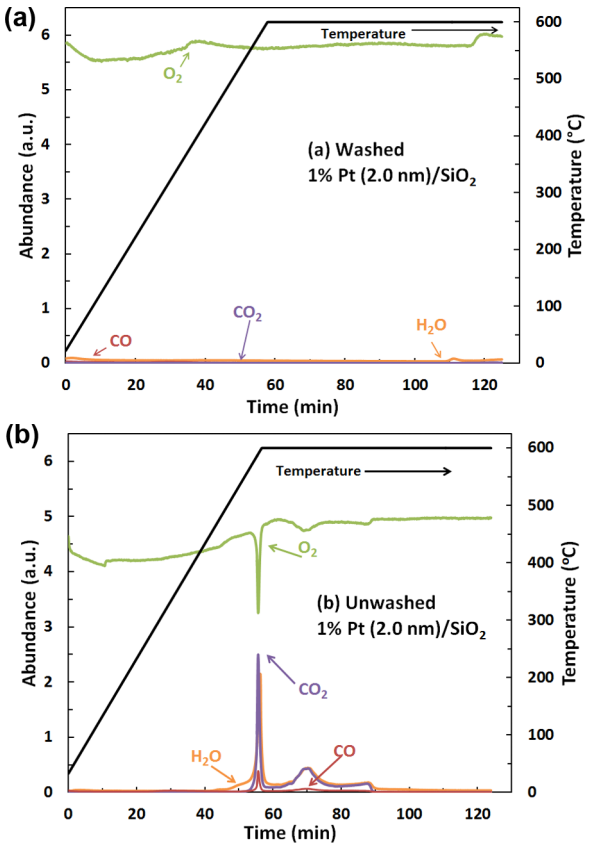

Figure 3. TPO profiles for (a) washed 1% Pt (2 nm)/SiO_2 and (b) unwashed 1% Pt (2 nm)/SiO_2. The lack of combustion products in the washed sample indicates successful washing of excess organic capping agents (PVP).

observed after washing. To illustrate the effective washing, these results were compared with those of a different sample of 2.0 Pt nanoparticles that were synthesized and directly immobilized on silica without washing. This sample is labeled as unwashed because the triple washing in ethanol–hexanes cycles were skipped. The TPO results (Figure 3b) indicate a sharp oxygen (m/z = 32) consumption peak just before the furnace reached 600 °C and continued while the temperature was held at 600 °C. Simultaneously, products including CO (m/z = 28), CO_2 (m/z = 44), and H_2O (m/z = 18) from polymer combustion formed. In comparing the TPO profiles for the washed and unwashed nanoparticles, it is evident that the washing protocols adhered to are effective in removal the polymer. A similar confirmation[22] of effective washing was found for the ~3 nm Pt/silica in previous work. For the unwashed 3.4 nm particles immobilized on silica, the peak combustion temperature was near 350 °C. In the present study, for unwashed 2.0 nm particles immobilized on silica, the peak

dx.doi.org/10.1021/cs300625m | ACS Catal. 2012, 2, 2626–2629

combustion temperature was slightly less than 600 °C. These size-dependent combustion results suggest a particle size dependence in which the polymer binds more strongly to the coordinately unsaturated surfaces of small particles more strongly than those of the large particles. A previous study[23] found that PVP binds to small Pd particles through its oxygen atom, but through both its nitrogen and oxygen atoms for large Pd particles. These results, along with the increase in uncoordinated surface sites for small particles compared with large particles, support the trend of the peak combustion temperature increasing with decreasing particle size.

2.2. Structure Sensitive Poisoning of a Catalytic Reaction. *Ethylene Hydrogenation without Sulfur Poisoning.* The ethylene hydrogenation rates over the four different sizes of Pt particles on silica are presented in Figure 4 (red

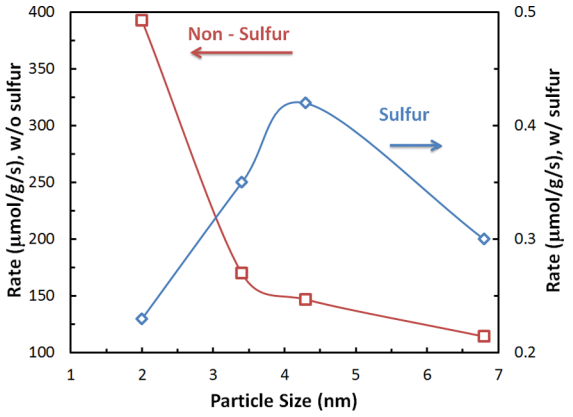

Figure 4. Ethylene hydrogenation rate per mass catalyst with and without a thiophene (sulfur) treatment prior to the reaction as a function of Pt particle size.

square symbols) and indicated a trend consistent with a structure-insensitive catalytic reaction. This trend is expected because a number of investigators have determined that ethylene hydrogenation is a structure-insensitive catalytic reaction.[21,24−27] Consequently, after normalization by the Pt loading and Pt dispersion, turnover frequencies (TOFs) in the range of 10.2−13.9 s^{-1} with an average (over the four particle sizes) of 12.3 s^{-1} were obtained (Figure 5, red square symbols). By correcting the reported[28] TOF for the Pt(111) single crystal to the temperature (40 °C) of the present study using an

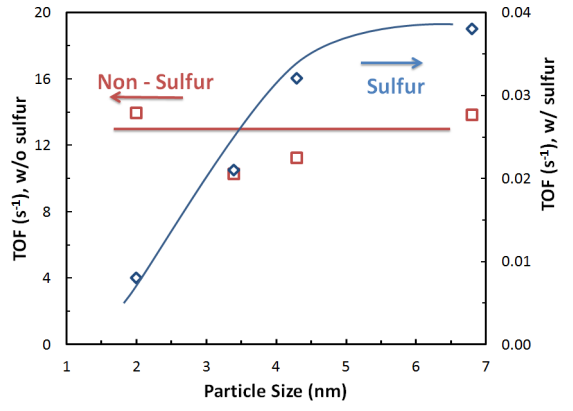

Figure 5. Ethylene hydrogenation TOF with and without a thiophene (sulfur) treatment prior to the reaction as a function of Pt particle size.

activation energy of 8 kcal/mol (a common value[29,30]), the expected TOF would be 16.8 s^{-1}. A similar value (16.6 s^{-1}) is obtained by correcting an average of values in the literature[20,24,25,28,30−34] over various Pt catalysts at room temperature to a temperature of 40 °C. These values are slightly higher than the ones measured in this study. Using an existing method of ethylene hydrogenation TOFs as a quantitative tool for determining the active Pt surface area,[20] an average of 75% (over the 4 particle sizes) of the Pt sites. In addition, dispersions were calculated from the traditionally accepted hemispherical shape, whereas the TEM images show mainly spherical shapes. Assuming the ethylene hydrogenation approach as accurate, these geometric contributions likely caused the Pt surface area to be lower than expected; however, the general trends for the ethylene hydrogenation TOF and rates normalized per mass of catalyst are consistent with the expectations for Pt particles of 2−7 nm immobilized on silica.

Ethylene Hydrogenation with Sulfur Poisoning. The ethylene hydrogenation rates after thiophene poisoning over the four different sizes of Pt particles on silica indicate that the thiophene exposure caused a large loss in activity (Figure 4, blue diamonds). Without the thiophene poisoning, the ethylene hydrogenation rates were between 350 and 1700 times more active when compared with after the poisoning. Moreover, the rate per mass of catalyst now proceeded through a maximum with the 4.3 nm Pt particles. Analogously, after normalizing per the same number of surface Pt sites as for ethylene hydrogenation without thiophene poisoning, the TOF increased with increasing particle size (Figure 5). TEM images (4.3 nm Pt/silica catalyst, Figure 6) verified negligible effects of the thiophene treatment (the highest temperature) on the catalysts.

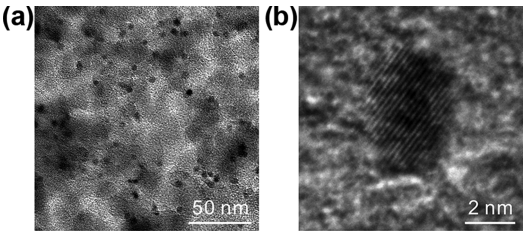

Figure 6. TEM images of the 5 nm Pt/silica catalyst after sulfidation at T = 150 °C.

The trends of Figures 4 and 5 are consistent with a mechanism involving a strong binding adsorbate,[35,36] which would be thiophene as a catalytic poison in this case. The more intrinsically active surfaces of large Pt particles, as compared with surfaces of small Pt particles, follows recently published results by the Iglesia group,[8] which demonstrated the weaker Pt−S bonds at the surface of large particles led to more sulfur surface vacancies and, consequently, more direct desulfurization and hydrogenation activity than the surfaces of small Pt surfaces containing much stronger Pt−S bonds. This finding is interesting because a poison was used to convert a structure-insensitive-catalyzed reaction into a structure-sensitive one.

Assuming that the turnover rate of an available Pt site does not change with a neighbor site being blocked by thiophene, the available Pt surface sites can be estimated by the ethylene hydrogenation rate. Using the nonthiophene-poisoned ethylene hydrogenation TOF rates to titrate the Pt surface sites not blocked by thiophene following poisoning, a range of 0.05−

dx.doi.org/10.1021/cs300625m | ACS Catal. 2012, 2, 2626−2629

0.23% (increasing with increasing particle size) of the Pt surface sites contributes to the ethylene hydrogenation turnover. Using an existing model[37] for kinetic analysis of particle size effects through adsorption strength differences on coordinatively unsaturated (edge) and coordinatively saturated (terrace) surfaces, the thiophene adsorption strength difference on edges as compared with terraces would be ~31.7 kJ/mol.

For comparative purposes, the Iglesia group has reported thiophene HDS TOFs in the ranges (depending on particle size and H_2S pressure) of 0.03−0.3 s^{-1} for Pt/silica at T = 300 °C[8] and 0.05−0.2 s^{-1} Ru/silica at T = 350 °C.[15] The TOFs for pyrrole hydrogenation over a similar set of Pt particles of SBA-15 were on the order of 0.06 s^{-1} at a temperature of 140 °C.[21] These values are lower than ethylene hydrogenation,[24,25,28,30−34] benzene hydrogenation,[38,39] and cyclohexene hydrogenation,[27,40] which occur at similar or lower (in the case of ethylene hydrogenation) temperatures. However, the TOFs for pyrrole hydrogenation are 2 orders of magnitude higher than the thiophene-poisoned ethylene hydrogenation TOF in the current study. The comparison of these turnover rate values and the corresponding temperatures indicate the strong poisoning effects of sulfur- and nitrogen-based organics.

CONCLUSION

This study represents the concept of poison-induced structure sensitivity into catalytic reactions, which was achieved using colloidal strategies to synthesize distinct sizes of monodisperse Pt nanoparticles in the important size range for structure sensitivity studies (2−7 nm). This effort is part of a broader study in which structure sensitivity is analyzed in complex reactions in which reactants and poisons may contribute the particle size dependence. The use of colloidal chemistry to synthesize well-defined particle morphologies permits fine-tuning the catalysis properties as compared with other strategies that yield broad particle size distributions that may mask underlying catalytic phenomena.

ASSOCIATED CONTENT

Supporting Information

Experimental procedures. This material is available free of charge via the Internet at http://pubs.acs.org.

AUTHOR INFORMATION

Corresponding Author

*Phone: (813) 974-6498. E-mail: jnkuhn@usf.edu.

Notes

The authors declare no competing financial interest.

ACKNOWLEDGMENTS

Funding for this work from USF, in part through the USF Internal Awards Program under Grant No. 0074332, is gratefully acknowledged. Assistance from the Nanotechnology and Research Education Center (NREC) within the College of Engineering at USF is also appreciated.

REFERENCES

(1) Bartholomew, C. H.; Farrauto, R. J. *Fundamentals of Industrial Catalytic Processes*, 2nd ed.; John Wiley & Sons: New York, 2006.
(2) Kuo, Y.-J.; Tatarchuk, B. J. *J. Catal.* **1988**, 229−249.
(3) Vit, Z.; Cinibulk, J.; Gulkova, D. *Appl. Catal.* **2004**, 99−107.
(4) Cooper, B. H.; Donnis, B. B. L. *Appl. Catal., A* **1996**, *137*, 203−223.
(5) Kuhn, J. N. *Catalysis* **2010**, *23*, 96−138.
(6) Reinhoudt, H. R.; Troost, R.; van Langeveld, A. D.; Sie, S. T.; van Veen, J. A. R.; Moulijn, J. A. *Fuel Process. Technol.* **1999**, *61*, 133−147.
(7) Sun, Y.; Prins, R. *Angew. Chem., Int. Ed.* **2008**, *47*, 8478−8481.
(8) Wang, H.; Iglesia, E. *ChemCatChem* **2011**, *3*, 1166−1175.
(9) Prins, R.; Egorova, M.; Rothlisberger, A.; Zhao, Y.; Sivasankar, N.; Kukula, P. *Catal. Today* **2006**, *111*, 84−93.
(10) Breysse, M.; Djega-Mariadassou, G.; Pessayre, S.; Geantet, C.; Vrinat, M.; Perot, G.; Lemaire, M. *Catal. Today* **2003**, *84*, 129−138.
(11) Knudsen, K. G.; Cooper, B. H.; Topsoe, H. *Appl. Catal., A* **1999**, *189*, 205−215.
(12) Breysse, M.; Afanasiev, P.; Geantet, C.; Vrinat, M. *Catal. Today* **2003**, *86*, 5−16.
(13) Matsui, T.; Harada, M.; Ichihashi, Y.; Bando, K. K.; Matsubayashi, N.; Toba, M.; Yoshimura, Y. *Appl. Catal., A* **2005**, *286*, 249−257.
(14) Reinhoudt, H. R.; Troost, R.; van Schalkwijk, S.; van Langeveld, A. D.; Sie, S. T.; van Veen, J. A. R.; Moulijn, J. A. *Fuel Process. Technol.* **1999**, 117−131.
(15) Wang, H.; Iglesia, E. *J. Catal.* **2010**, *273*, 245−256.
(16) Niquille-Röthlisberger, A.; Prins, R. *Catal. Today* **2007**, *123*, 198−207.
(17) Reyes, P.; Pecchi, G.; Morales, M.; Fierro, J. L. G. *Appl. Catal., A* **1997**, *163*, 145−152.
(18) Guo, H.; Sun, Y.; Prins, R. *Catal. Today* **2008**, *130*, 249−253.
(19) Wang, Y.; Ren, J.; Deng, K.; Gui, L.; Tang, Y. *Chem. Mater.* **2000**, *12*, 1622−1627.
(20) Kuhn, J. N.; Tsung, C.-K.; Huang, W.; Somorjai, G. A. *J. Catal.* **2009**, *265*, 209−215.
(21) Kuhn, J. N.; Huang, W.; Tsung, C.-K.; Zhang, Y.; Somorjai, G. A. *J. Am. Chem. Soc.* **2008**, *130*, 14026−14027.
(22) Blavo, S. O.; Baldyga, L.; Sanchez, M. D.; Kuhn, J. N. *J. ASTM Int.* **2011**, *8*, 1−9.
(23) Xian, J.; Hua, Q.; Jiang, Z.; Ma, Y.; Huang, W. *Langmuir* **2012**, *28*, 6736−6741.
(24) Schlatter, J. C.; Boudart, M. *J. Catal.* **1972**, *24*, 482−492.
(25) Cortright, R. D.; Goddard, S. A.; Rekoske, J. E.; Dumesic, J. A. *J. Catal.* **1991**, *127*, 342−353.
(26) Dorling, T. A.; Eastlake, M. J.; Moss, R. L. *J. Catal.* **1969**, *14*, 23−33.
(27) McCrea, K. R.; Somorjai, G. A. *J. Mol. Catal. A: Chem.* **2000**, *163*, 43−53.
(28) Zaera, F.; Somorjai, G. A. *J. Am. Chem. Soc.* **1984**, *106*, 2288−2293.
(29) Rioux, R. M.; Song, H.; Hoefelmeyer, J. D.; Yang, P.; Somorjai, G. A. *J. Phys. Chem. B* **2005**, *109*, 2192−2202.
(30) Song, H.; Rioux, R. M.; Hoefelmeyer, J. D.; Komor, R.; Niesz, K.; Grass, M.; Yang, P.; Somorjai, G. A. *J. Am. Chem. Soc.* **2006**, *128*, 3027−3037.
(31) Backman, A. L.; Masel, R. I. *J. Vac. Sci. Technol.* **1988**, *6*, 1137−1139.
(32) Ford, L. P.; Nigg, H. L.; Blowers, P.; Masel, R. I. *J. Catal.* **1998**, *179*, 163−170.
(33) Contreras, A. M.; Grunes, J.; Yan, X.-M.; Liddle, A.; Somorjai, G. A. *Catal. Lett.* **2005**, *100*, 115−124.
(34) Grunes, J.; Zhu, J.; Anderson, E. A.; Somorjai, G. A. *J. Phys. Chem. B* **2002**, *106*, 11463−11468.
(35) Van Santen, R. A. *Acc. Chem. Res.* **2009**, *42*, 57−66.
(36) Che, M.; Bennett, C. O. *Adv. Catal.* **1989**, *36*, 55−172.
(37) Murzin, D. Y. *J. Catal.* **2010**, *276*, 85−91.
(38) Bratlie, K. M.; Lee, H.; Komvopoulos, K.; Yang, P.; Somorjai, G. A. *Nano Lett.* **2007**, *7*, 3097−3101.
(39) Bratlie, K. M.; Montano, M. O.; Flores, L. D.; Paajanen, M.; Somorjai, G. A. *J. Am. Chem. Soc.* **2006**, *128*, 12810−12816.
(40) Rioux, R. M.; Hsu, B. B.; Grass, M. E.; Song, H.; Somorjai, G. A. *Catal. Lett.* **2008**, *126*, 10−19.